

**Biophysical Journal, Volume 116**

**Supplemental Information**

**KRAS Prenylation Is Required for Bivalent Binding with Calmodulin in a Nucleotide-Independent Manner**

**Constance Agamasu, Rodolfo Ghirlando, Troy Taylor, Simon Messing, Timothy H. Tran, Lakshman Bindu, Marco Tonelli, Dwight V. Nissley, Frank McCormick, and Andrew G. Stephen**

**Table S1:** Characterization of components studied by sedimentation velocity

**Table S2:** Summary of binding parameters obtained of CaM binding to GDP-bound KRAS4b variants via SV-AUC, SPR and ITC

**Table S3.** Summary of binding affinities obtained for CaM binding to various KRAS4b constructs via ITC

**Figure S1.** *Unprenylated GDP and GNP-bound KRAS4b do not interact with CaM* (A) Sedimentation velocity absorbance  $c(s)$  profiles obtained for individual CaM and KRAS4b variants at 70  $\mu\text{M}$  CaM (cyan) and  $\sim 10$   $\mu\text{M}$  GDP and GNP-bound KRAS4b-FMe, KRAS4b 2-185 and KRAS4b 2-169. (B) Sedimentation velocity absorbance  $c(s)$  profiles for mixtures of 30  $\mu\text{M}$  CaM and 20  $\mu\text{M}$  GDP and GNP-bound KRAS4b constructs as indicated. Faster sedimenting species was only observed for CaM and GDP and GNP-bound KRAS4b-FMe. (C) ITC heat of dilution data acquired upon injection of buffer into 30  $\mu\text{M}$  KRAS4b-FMe and 1 mM CaM into buffer. (D) ITC data obtained for CaM (1 mM) titrated into GDP and GNP-bound KRAS4b 2-185 (30  $\mu\text{M}$ ).

**Figure S2.** *Prenylated GDP and GNP-bound KRAS4b-FMe forms a 2:1 complexes with CaM.* Absorbance (top panel) and interference (bottom panel) sedimentation velocity  $c(s)$  profiles for the titration of (A) CaM into 6  $\mu\text{M}$  GDP-bound KRAS4b-FMe, CaM into 3  $\mu\text{M}$  GDP-bound KRAS4b-FMe, and GDP-bound KRAS4b-FMe into 6  $\mu\text{M}$  CaM, (B) CaM-C into 3  $\mu\text{M}$  GDP-bound KRAS4b-FMe and (C) CaM-N into 3  $\mu\text{M}$  GDP-bound KRAS4b-FMe at the concentrations indicated. The weighted-average sedimentation coefficient  $S_w$  used for analysis in Figure 2 is obtained by integration of the  $c(s)$  profiles shown.

**Figure S3.** *NMR data further supports that unprenylated GDP and GNP-bound KRAS4b do not interact with CaM.* 2D  $^1\text{H}$ - $^{15}\text{N}$  HSQC of  $^{15}\text{N}$ -labeled GDP and GNP-bound KRAS4b2-185 at 50  $\mu\text{M}$  titrated with 500  $\mu\text{M}$  CaM. Again, no CSP or line broadening was observed between unprenylated KRAS4b and CaM.

**Figure S4.** *NMR data of GDP-bound KRAS4b-FMe binding to CaM-C and CaM-N.* (A) 2D  $^1\text{H}$ - $^{15}\text{N}$  HSQC of  $^{15}\text{N}$ -labeled CaM-N titrated with GDP-bound KRAS4b-FMe at a 1.5:1 ratio. (B) 2D  $^1\text{H}$ - $^{15}\text{N}$  HSQC of  $^{15}\text{N}$ -labeled CaM-C titrated with GDP-bound KRAS4b-FMe at a 1.5:1 ratio. (C-D) A histogram of normalized  $^1\text{H}$ - $^{15}\text{N}$  chemical shift changes vs. residue number calculated from the HSQC spectra for CaM-N and CaM-C upon addition of GDP-bound KRAS4b-FMe. (E-F) Cartoon representation of CaM structure (PDB ID: 3CLN) highlighting residues that exhibited substantial ( $>0.05$  ppm) chemical shift changes for CaM-N (red) or CaM-C (magenta).

**Figure S5.** *NMR data further supports that unprenylated GDP and GNP-bound KRAS4b do not interact with CaM.* 2D  $^1\text{H}$ - $^{15}\text{N}$  HSQC of  $^{15}\text{N}$ -labeled CaM at 50  $\mu\text{M}$  titrated with 500  $\mu\text{M}$  upon titration of unprenylated KRAS4b into CaM.

**Figure S6.** *KSKTKC-FMe does not induce secondary structural rearrangements in CaM.* FarUV circular dichroism spectra obtained for CaM (magenta) and the KSKTKC-FMe: CaM complex (green).

**Table S1:** Characterization of components studied by sedimentation velocity.

Component	Concentration studied ( $\mu\text{M}$ )	$S_{20,w}$ (S)	$M$ (kDa)
CaM	70	2.0	18
CaM-N	110	1.4	10
CaM-C	25	1.5	13
GDP KRAS4b-FMe	10	2.2	23
GNP KRAS4b-FMe	10	2.2	22
GDP KRAS4b 2-185	10	2.2	23
GNP KRAS4b 2-185	10	2.2	23
GDP KRAS4b 2-169	10	2.2	21
GNP KRAS4b 2-169	10	2.3	21
MSP1D1 POPC:POPS 70:30 Nanodisc	4.5	3.1	84

**Table S2:** Summary of binding parameters obtained of CaM binding to GDP-bound KRAS4b variants via SV-AUC, SPR and ITC

Technique	Sample 1	Sample 2	Kd ( $\mu\text{M}$ )	$\Delta\text{H}$ (kcal/mol)	$-\text{T}\Delta\text{S}$ (kcal/mol)	$\Delta\text{G}$ (kcal/mol)
SV-AUC	CaM	KRAS4b-FMe	Co-Op*			
SV-AUC	CaM-C	KRAS4b-FMe	$0.4 \pm 0.1$			
SV-AUC	CaM-N	KRAS4b-FMe	$4 \pm 1$			
SPR	CaM	KRAS4b-FMe	$0.4 \pm 0.1$			
SPR	CaM-C	KRAS4b-FMe	$0.6 \pm 0.1$			
SPR	CaM-N	KRAS4b-FMe	$3 \pm 0.2$			
ITC	CaM	KRAS4b-FMe	$0.3 \pm 0.1$			
ITC	CaM-C	KRAS4b-FMe	$0.5 \pm 0.1$	$-5.1 \pm 0.3$	-3.5	-8.6
ITC	CaM-N	KRAS4b-FMe	$4 \pm 1$	$-7.3 \pm 0.5$	-0.2	-7.5

Co-op\* Data were modeled in terms of two non-symmetric sites with microscopic binding constants. The microscopic binding constants observed for binding to CaM-N and CaM-C were applied and fixed to obtain a favorable co-operative term.

**Table S3:** Summary of binding affinities obtained for CaM binding to various KRAS4b constructs via ITC

Cell	Syringe	$K_d$
KRAS4b-FMe (44 $\mu$ M)	CaM (120 $\mu$ M)	0.3 $\mu$ M $\pm$ 0.08 $\mu$ M
KRAS4b-FMe (30 $\mu$ M)	CaM-C (300 $\mu$ M)	0.5 $\mu$ M $\pm$ 0.07 $\mu$ M
KRAS4b-FMe (30 $\mu$ M)	CaM-N (500 $\mu$ M)	4 $\mu$ M $\pm$ 1 $\mu$ M
KRAS4b-Farnesyl (57 $\mu$ M)	CaM (300 $\mu$ M)	2 $\mu$ M $\pm$ 0.2 $\mu$ M
KRAS4b-2-180-AAAAC-Farnesyl (48 $\mu$ M)	CaM (440 $\mu$ M)	10 $\mu$ M $\pm$ 1 $\mu$ M
HVR-FMe (50 $\mu$ M)	CaM (150 $\mu$ M)	0.3 $\mu$ M $\pm$ 0.06 $\mu$ M
KSKTKC-FMe (50 $\mu$ M)	CaM (130 $\mu$ M)	0.4 $\mu$ M $\pm$ 0.1 $\mu$ M
KSKTKC-GMe (30 $\mu$ M)	CaM (200 $\mu$ M)	3 $\mu$ M $\pm$ 0.01 $\mu$ M
KSKTKC-PMe (30 $\mu$ M)	CaM (800 $\mu$ M)	30 $\mu$ M $\pm$ 3 $\mu$ M
GDP KRAS4b 2-185 (30 $\mu$ M)	CaM (1 mM)	ND *
GNP KRAS4b 2-185 (30 $\mu$ M)	CaM (1 mM)	ND *

ND\* No binding detected.

Figure S1

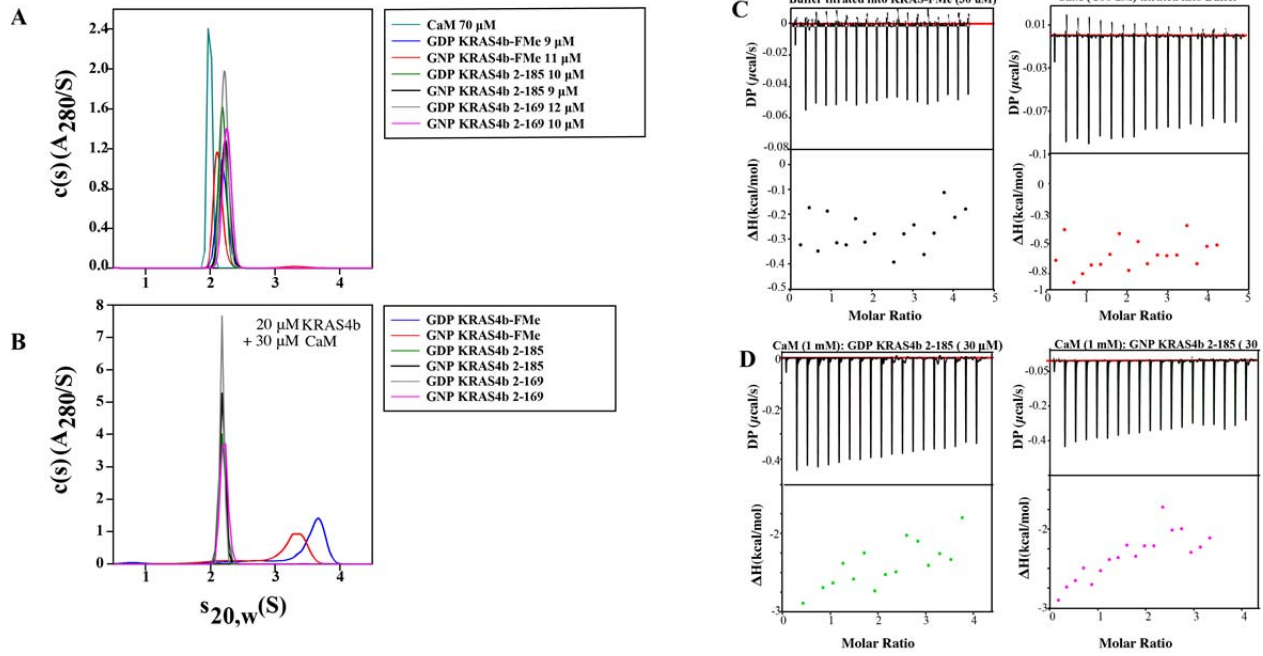


Figure S2

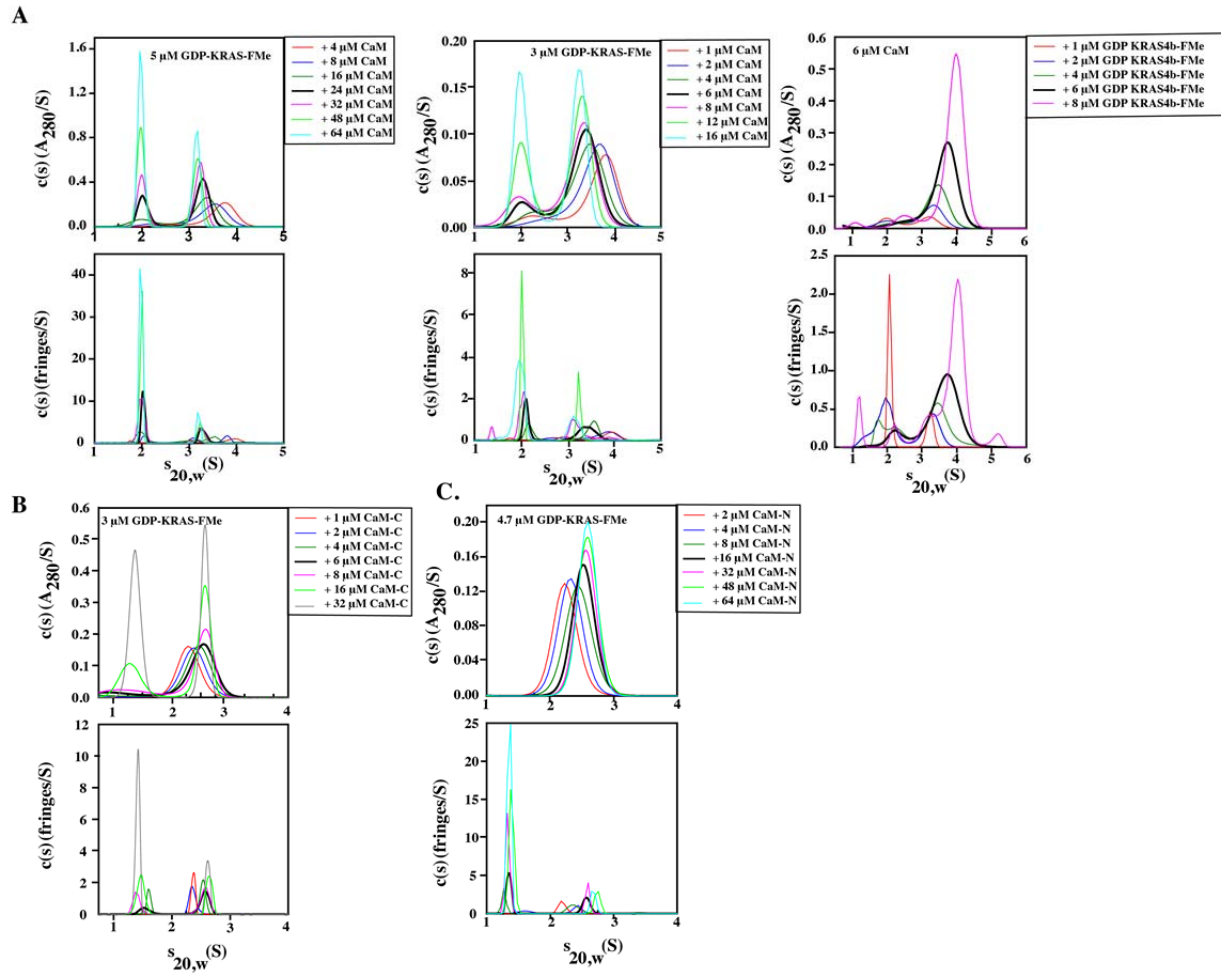


Figure S3

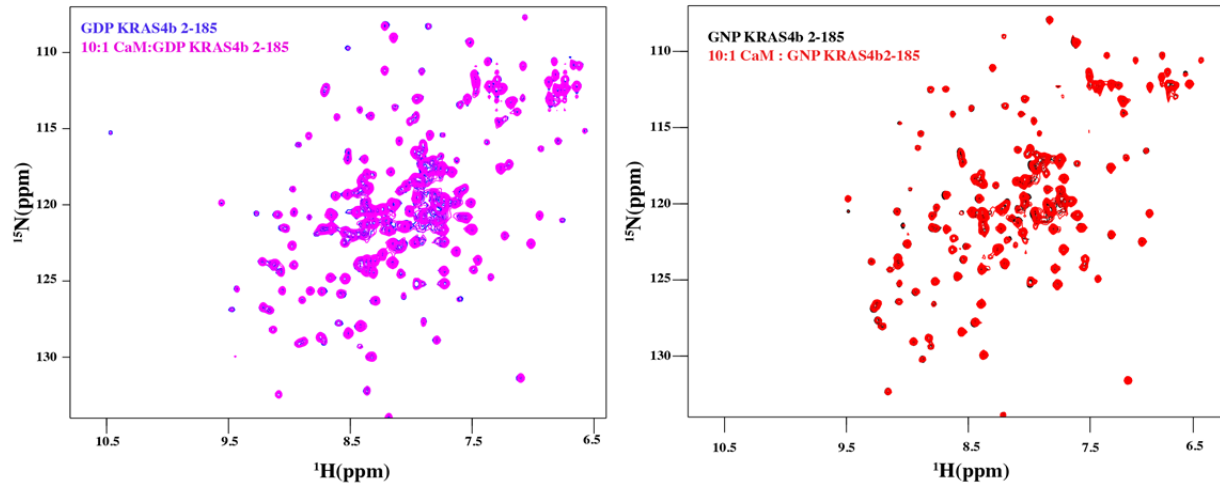




Figure S4

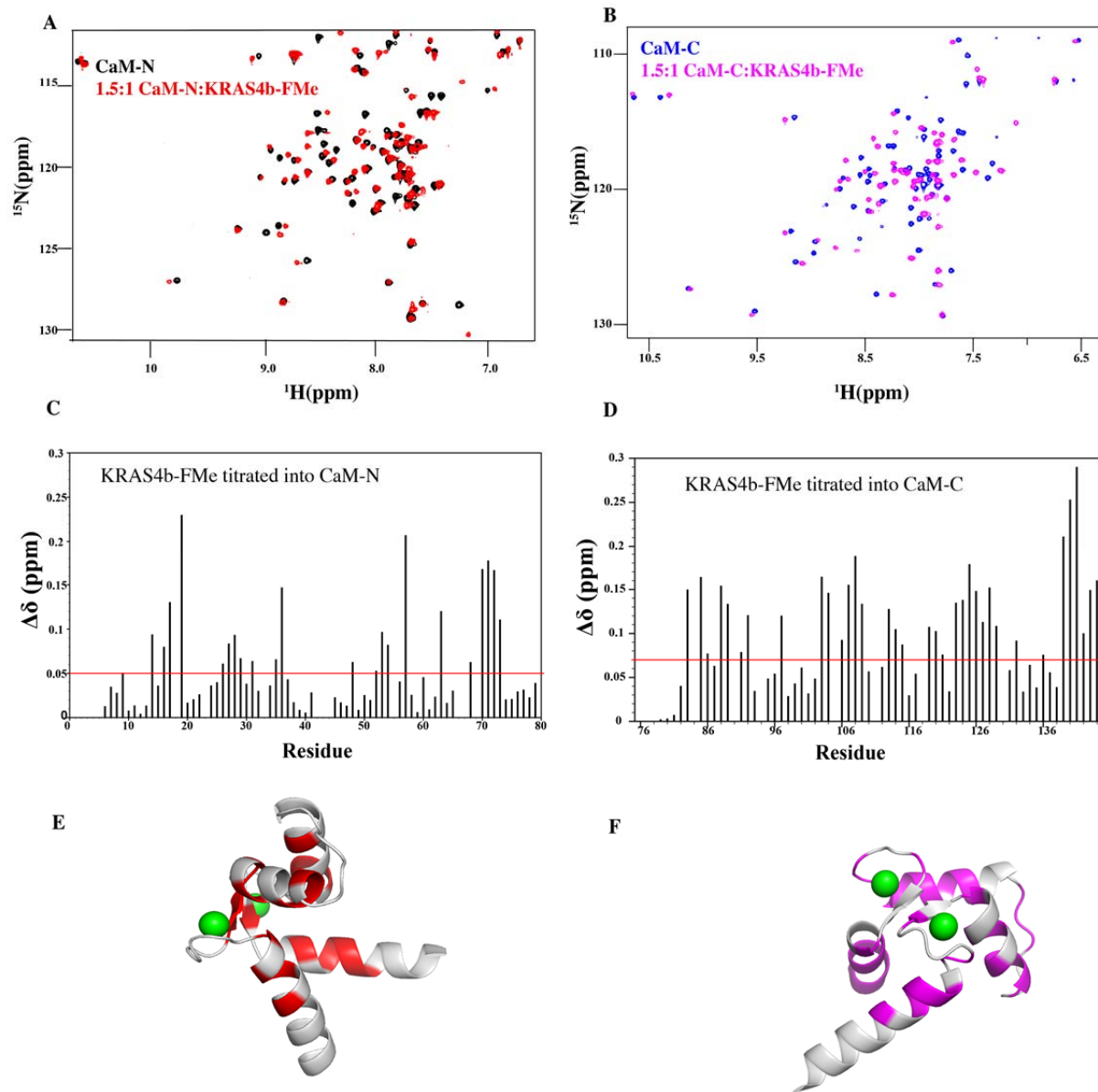


Figure S5

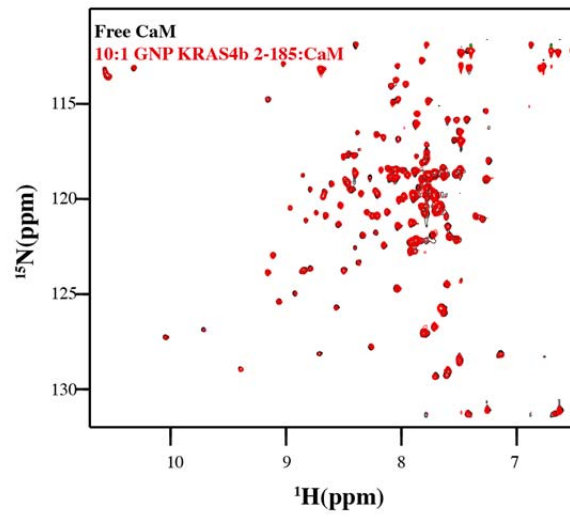
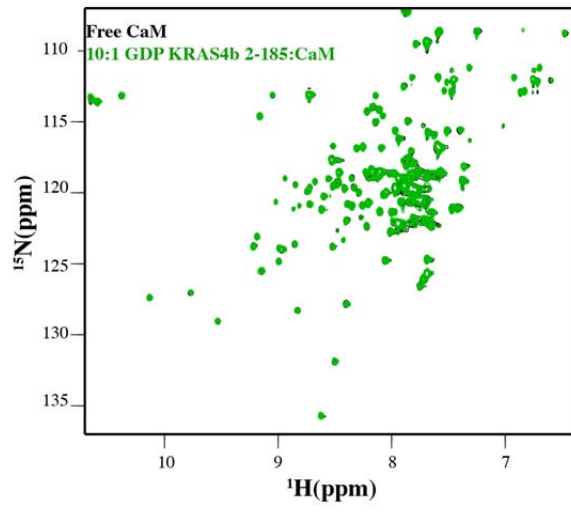


Figure S6

